Alpha-mangostin reduces mechanical stiffness of various cells

Thi Kieu Trang Phan, Fahimeh Shahbazzadeh, Takanori Kihara*

Department of Life and Environment Engineering, Faculty of Environmental Engineering, The University of Kitakyushu, 1-1 Hibikino, Wakamatsu, Kitakyushu, Fukuoka 808-0135, Japan.

*Corresponding author. Tel: +81-93-695-3290, Fax: +81-93-695-3368

E-mail address: tkihara@kitakyu-u.ac.jp (T. Kihara)

Abstract

Alpha-mangostin (α-mangostin) has been identified as a naturally occurring compound with potential anticancer properties. It can induce apoptosis and inhibit the growth and metastasis of cancer cells. Moreover, α-mangostin reduces the mechanical stiffness of lung cancer cells. The objective of this study was to determine the effect of α-mangostin on the mechanical stiffness of various cells, as well as cell viability. The following cell types were examined: human fibroblast TIG-1 cells, human cancerous HeLa cells, human embryonic kidney HEK293 cells, mouse macrophage RAW 264.7 cells, and human myeloblasts KG-1 cells. Cells were treated with α-mangostin, and then examined for cell viability, actin cytoskeletal structures, and surface mechanical stiffness using atomic force microscopy. α-Mangostin demonstrated cytotoxicity against TIG-1, HeLa, HEK293, and KG-1 cells, but not against RAW 264.7 cells. The cytotoxic effect of α-mangostin varies according to cell type. On the other hand, α-mangostin reduced the mechanical stiffness of all cell types, including RAW 264.7 cells. Upon treatment with α-mangostin, F-actin was slightly reduced but the actin cytoskeletal structures were little altered in these cells. Thus, reducing mechanical stiffness of animal cells is an inherent effect of α-mangostin. Our results show that α-mangostin is a naturally occurring compound with potential to change the actin cytoskeletal micro-structures and reduce the surface stiffness of various cells.

Keywords

α-mangostin; cell mechanics; cytotoxicity; atomic force microscopy; actin cytoskeleton

Introduction

α-Mangostin is one of the major xanthone compounds extracted from the pericarp of mangosteen (*Garcinia mangostana* Linn.) fruit. It has been demonstrated to possess numerous bioactive functions, both *in vitro* and *in vivo,* against various diseases, including cancer, inflammation, allergy, and bacterial and viral infections [1]. α-Mangostin targets different cellular factors through various mechanisms such as inducing apoptosis in cancer cells by regulating Bcl-2, Bax, and p53 [2-4]; preventing the metastatic activities of cancer cells via inhibition of MMP-2, MMP-9, and NF-κB [5-7]; and directly scavenging reactive oxygen species (ROS), thereby preventing neurotoxicity and ROS production by 3-nitropropionic acid in cultured neurons [8]. Furthermore, recent research has illustrated that α-mangostin reduces cell surface stiffness in lung cancer cells [9].

Cell surface stiffness is attributed to the actin cytoskeleton [10-13], and reflects the cell surface actin architectures [14, 15]. Moreover, cell surface stiffness changes in accordance with cellular events related to the remodeling of the actin cytoskeleton [16-19]. Therefore, analyzing cell surface stiffness may reveal changes of cell characteristics, and provide a better understanding of the actin cytoskeleton remodeling process in certain cellular events and disease states. Atomic force microscopy (AFM) is one of the most sensitive techniques for examining cell mechanics under physiological conditions [20]. AFM contains a nano-sized probe which can determine cell surface stiffness by indentation [21, 16]. This method is used to analyze surface stiffness of both adherent cells and suspension cells [22, 16, 23-25, 19]. Thus, AFM can be a powerful tool for analyzing the mechanical stiffness and actin cytoskeleton states of various cells.

We recently reported that α-mangostin suppressed the subsistence, migration, and invasion of lung cancer cells [9]. In that study, we demonstrated that α-mangostin decreased the cell surface stiffness of lung cancer A549 cells and lung normal fibroblast-like CCD-14Br cells. Of these two cell types, the surface stiffness of A549 cells decreased significantly when treated with α-mangostin [9]. The mechanical changes in cancer cells are important indicators of cancer state and type: softer cancer cells show more invasive properties [26, 27]; apoptotic cancer cells are softened [28, 29]. Is the α-mangostin-induced reduction of

surface stiffness in A549 cells related to the effects of α-mangostin on cancer cells? To answer this question, we have to first identify the range of cells on which α-mangostin has an effect, and then to elucidate the mechanism of how α-mangostin reduces the surface stiffness of these cancer cells.

In the present study, we examined the cell types that were affected by α-mangostin with respect to cell surface stiffness. Identifying the range of cells that are impacted by the action of α-mangostin may help us to elucidate the mechanism. We used different cell types including normal human fibroblast TIG-1 cells, human cervical cancer HeLa cells, human embryonic kidney HEK293 cells, mouse leukemia macrophage RAW 264.7 cells, and human leukemia myeloblasts KG-1 cells. TIG-1, HeLa, HEK293, and RAW 264.7 cells are adherent cells and KG-1 cells are suspension cells. The morphologies of these cells vary, and the features of the actin cytoskeleton vary in these cell types. TIG-1 cells have an elongated morphology; HeLa and HEK293 cells have a shortly extended morphology; RAW 264.7 cells have weakly adhering morphology; and KG-1 cells are suspended and spherical shape. We examined the sensitivity of these cells to α-mangostin and the effects of α-mangostin on cell mechanics, actin cytoskeleton, and cell viability.

Material and Methods

Materials

Human fetal lung normal fibroblast TIG-1 cells, human cervical cancer HeLa cells, and human embryonic kidney HEK293 cells were obtained from Japanese Collection of Research Bioresources (JCRB) cell bank (Osaka, Japan). Human leukemia myeloblast KG-1 cells and mouse leukemia macrophage RAW 264.7 cells were obtained from Riken Cell Bank (Ibaraki, Japan). α-Mangostin, rhodamine labeled-phalloidin, cytochalasin D, DMEM, and RPMI1640 medium were purchased from Wako Pure Chemical Industries Ltd. (Osaka, Japan). Cell anchoring molecule, SUNBRIGHT OE-020CS, was purchased from NOF Corporation (Tokyo, Japan). The cone probe (BL-AC-40TS-C2; spring constant: around 0.05 N/m) was purchased from Olympus (Tokyo, Japan). Cell counting kit-8 was purchased from Dojindo Molecular Technologies, Inc. (Kumamoto, Japan). Cell harvesting solution TrypLE express and fetal bovine serum (FBS) were purchased

from Life Technologies Japan Ltd. (Tokyo, Japan). Antibiotics were purchased from Sigma-Aldrich (St. Louis, MO). Glass-based culture dishes were purchased from Matsunami Glass (Osaka, Japan). Other reagents were purchased from Sigma-Aldrich, Wako Pure Chemical Industries Ltd., or Life Technologies Japan Ltd.

Preparation of cell anchoring dishes

We coated cell anchoring molecule, SUNBRIGHT OE-020CS, on the culture dishes as described previously [14]. Briefly, the polystyrene tissue culture dishes were coated with BSA, and then the surfaces were coated with SUNBRIGHT OE-020CS. SUNBRIGHT OE-020CS contains an oleyl group at one end and keeps a floating cell on the coated dish [30]. The anchored cells are fixed, and then the cell surface stiffness can be measured by AFM [25, 19].

Cell culture

TIG-1, HeLa, HEK293, and RAW 264.7 cells were cultured in DMEM containing 10% FBS and antibiotics (100 units/mL penicillin G and 100 μg/mL streptomycin sulfate), and KG-1 cells were cultured in RPMI1640 medium containing 10% FBS and the antibiotics in humidified atmosphere of 95% air and 5% CO_2 at 37°C.

Cytotoxicity assay

The cytotoxicities of α-mangostin on various cells were evaluated by the cell counting kit-8 as recommended by the manufacturer. The adherent cells were seeded on a 96 well culture plate at 10^4 cells/well and cultured for 24 h, so as to allow the cells to adhere to the plate. The culture medium was replaced by 100 μL of fresh culture medium diluted with various concentrations of α-mangostin and cultured for further 24 h. The cell counting kit-8 solution (10 μL) was added to each well and incubated for 1 h. For KG-1 cells, the cells were seeded on a 96 well plate at 2×10^4 cells/well with 100 μL of culture medium containing with various concentrations of α-mangostin and cultured for 24 h. The cell counting kit-8 solution (10 μL) was added to each well and incubated for 2 h. The absorbance was then measured at 450 nm using a microplate reader. The

absorbance values were fitted with the below Hill equation.

$$f(x) = a + \frac{b-a}{1+\left(\frac{x}{h}\right)^r} \quad (1)$$

Where x = concentration of α-mangostin, h = value of EC_{50}, r = Hill coefficient, a = base value of the absorbance, b = top value of the absorbance.

AFM measurements

The cells were manipulated by AFM (Nanowizard III; JPK Instruments AG, Berlin, Germany) at room temperature. TIG-1, Hela, HEK293, and RAW 264.7 cells were cultured on normal culture dishes for 24 h and then treated with α-mangostin for 6 h. KG-1 cells were plated on the cell anchoring dishes for 1 h in serum free medium, then washed with PBS to remove unattached cells, and cultured for 6 h in α-mangostin containing complete culture medium. The cone shaped AFM probe was indented 25 different points within 1 μm × 1 μm of cell top with a loading force of up to 0.5 nN and velocity of 5 μm/s. Young's modulus of the cell surface was calculated with the Hertz model [31]; the force-indentation curve for a region up to about 1 μm of indentation was fitted using JPK data processing software (JPK instruments AG) as:

$$F = \frac{E}{1-\nu^2}\frac{2\tan\alpha}{\pi}\delta^2 \quad (2)$$

Where F = force, δ = depth of the probe indentation, ν = Poisson's ratio (0.5), α = half-angle of the cone probe (9°), and E = Young's modulus. The median value adopted for the Young's modulus of each cell [23]. More than 21 cells and 525 force-distance curves were analyzed in each condition.

Actin filaments staining

TIG-1, Hela, HEK293, and RAW 264.7 cells were cultured on normal glass base dishes for 24 h and then treated with 10 μM α-mangostin for 6 h or 2 μg/mL cytochalasin D for 1.5 h. KG-1 cells were plated on the cell anchoring glass base dishes for 1 h in serum free medium, then washed with PBS to remove unattached cells, and cultured for 6 h in 10 μM α-mangostin or for 1.5 h in 2 μg/mL cytochalasin D containing complete culture medium. The cultured cells were fixed with 4% paraformaldehyde, permeabilized with 0.3% Triton

X-100, and then stained with rhodamine labeled-phalloidin for actin filaments. Specimens were observed by fluorescence microscopy (IX81, Olympus).

Statistical analysis

The logarithmic Young's modulus values for each group were compared by one-way analysis of variance and Dunnett comparison test. *p*-Values of less than 0.01 were considered as statistically significant.

Results

Cytotoxic sensitivity to α-mangostin varies by cell type

Firstly, we examined the cytotoxic effects of α-mangostin on TIG-1, HeLa, HEK293, RAW 264.7, and KG-1 cells. TIG-1, HeLa, HEK293, and RAW 264.7 cells are adherent cells, and were seeded onto culture plates and pre-cultured for 24 h. They were then treated with α-mangostin for 24 h. KG-1 cells are suspension cells and were seeded onto culture plates and cultured with α-mangostin for 24 h. The survival cell number was evaluated by activity of living cells' mitochondrial tetrazolium reductase enzyme. α-Mangostin exhibited cytotoxic effects on TIG-1, HeLa, HEK293, and KG-1 cells at a concentration of 100 μM (Fig. 1). On the other hand, α-mangostin did not affect the cell viability of RAW 264.7 cells even at the concentration of 100 μM (Fig. 1). This result is in agreement with that of a previous study by Chen et al. [32]. In Chen's study, the xanthones from mangosteen extracts, whose major component was α-mangostin, demonstrated no cytotoxicity on RAW 264.7 cells. The half-maximal effective concentration (EC_{50}) values of α-mangostin for the cytotoxicity of TIG-1, HeLa, HEK293, and KG-1 cells were estimated as 13, 16, 30, and 7.5 μM, respectively (Fig. 1). KG-1 cells were relatively sensitive but HEK293 cells were relatively resistant to the cytotoxic effects of α-mangostin. Thus, α-mangostin demonstrated cytotoxic effects on a number of different adherent cells and suspension leukemia myeloblasts. However, RAW 264.7 cells proved to be resistant to the cytotoxic effects of α-mangostin.

α-Mangostin reduces mechanical stiffness of various cells

Our previous study showed that α-mangostin suppressed the subsistence and decreased the mechanical properties of A549 cancer and CCD-14Br normal cells [9]. Mechanical changes caused by α-mangostin appeared within 6 h, which was before the onset of cytotoxic effects [9]. We examined the impact of α-mangostin on cell mechanics in TIG-1, HeLa, HEK293, RAW 264.7, and KG-1 cells. These cells were exposed to α-mangostin for 6 h after which surface stiffness was examined using AFM. The morphologies of these cells are shown in Fig. 2. TIG-1, HeLa, and HEK293 cells adhered and extended on the dish. TIG-1 cells in particular showed a highly elongated morphology (Fig. 2). While these cells remained extended after the 6 h α-mangostin treatment, HeLa and HEK293 cells appeared somewhat shrunken (Fig. 2). RAW 264.7 cells adhered but did not extend significantly, and after treatment with α-mangostin for 6 h, their morphology appeared unchanged (Fig. 2). KG-1 cells were fixed on cell anchoring dishes to measure their surface stiffness using AFM. The morphology of KG-1 cells was spherical and they were unchanged by treatment with α-mangostin (Fig. 2).

The distribution of the elastic modulus (Young's modulus) of these cells is shown in Fig. 3. The values of Young's modulus are plotted in logarithmic scale as they were distributed in a log-normal pattern [25]. With regard to the controls, the log-average values of the Young's moduli of TIG-1, HeLa, HEK293, RAW 264.7, and KG-1 cells were 5.4, 2.0, 0.28, 0.84, and 1.0 kPa, respectively (Fig. 3). TIG-1 fibroblasts had the highest surface stiffness of the cells tested, while HEK293 cells had the lowest. This result complements the data from our previous studies [25, 14, 15]. The surface stiffness of suspension KG-1 myeloblasts was higher than that of adhered HEK293 and RAW 264.7 cells (Fig. 3). Thus, it appears that the actin cytoskeleton near the plasma membrane mechanically supports the surface of spherical KG-1 cells.

The Young’s modulus of these cells reduced following α-mangostin treatment (Fig. 3). The Young’s modulus of normal fibroblast TIG-1 cells was slightly reduced from 5.4 to 3.3 kPa following treatment with 10 μM of α-mangostin (Fig. 3). The Young’s modulus of cancerous HeLa cells was markedly reduced from 2.0 to 0.68 kPa following treatment with 10 μM of α-mangostin (Fig. 3). This result demonstrates a similar

trend to our previous analysis, such that normal fibroblast-like CCD-14Br cells softened slightly, and lung cancer A547 cells softened significantly following treatment with α-mangostin [9]. The Young's modulus of HEK293 cells was too low and they had few mechanically supporting actin cytoskeletons, resulting in only a slight softening after treatment with α-mangostin (Fig. 3). RAW 264.7 cells, whose Young's modulus was relatively low, and which were resistant to the cytotoxic effects of α-mangostin, were also slightly softened by treatment with 10 and 20 μM α-mangostin (Fig. 3). Floating KG-1 cells, which had moderate stiffness and were sensitive to the cytotoxic effects of α-mangostin, were significantly softened by treatment with 5 and 10 μM α-mangostin (Fig. 3). Thus, although the impact of α-mangostin on cell mechanical properties varied by cell type, the mechanical stiffness of all cell types was reduced by the short-interval treatment with α-mangostin.

Actin cytoskeleton structures of α-mangostin-treated cells.

The mechanical stiffness of cells is largely attributed to the actin cytoskeleton [10-13]. Thus, the actin filaments of α-mangostin-treated cells were stained with rhodamine labeled-phalloidin and observed under the fluorescence microscope (Fig. 4). TIG-1 cells originally showed highly developed long actin stress fibers along the cell body. HeLa cells showed many weak actin fibers inside the cells and microvilli and protrusions on the edges. HEK293 and RAW 264.7 cells showed immature F-actin at the cell-cell border and many protrusions on the edges. KG-1 cells showed cortical F-actin and fine microvilli on the plasma membrane. Upon treatment with 10 μM α-mangostin, the F-actin amounts were slightly reduced and the actin cytoskeletal structures were little changed (Fig. 4). On the other hand, when these cells were treated with actin depolymerization reagent cytochalasin D, the F-actin structures were significantly distorted (Fig. 4). Especially, the actin structures of TIG-1, HeLa, and HEK293 cells were fully destroyed, and in KG-1 cells, the cortical actin almost vanished and F-actin aggregates appeared (Fig. 4). Thus, the mechanism of mechanical alteration by α-mangostin clearly differed from that of actin depolymerization reagent cytochalasin D. Probably α-mangostin is involved in changing the actin cytoskeletal micro-structures or

195 reducing the amount of the actin cytoskeleton gently, and then reduces the mechanical stiffness in various
196 cells.
197
198 **Discussion**
199 In this study, the results indicate that α-mangostin has cytotoxic effects on some of the cell types and the
200 ability to soften the mechanical properties of all the cell types that were analyzed. The impact of α-mangostin
201 on cell mechanical properties varied in different cell types, and the sensitivity results also varied from that of
202 the cytotoxic effect analysis.
203 First, we interpret our results from the perspective of actin cytoskeleton. The height of the value of
204 Young's modulus reflects the structure and state of the actin cytoskeleton present near the cell surface. TIG-1
205 cells have well-developed actin stress fibers, and their surface stiffness is highly enhanced due to the
206 developed actin stress fibers (Figs. 3 and 4). The surface stiffness of TIG-1 cells was slightly reduced and the
207 elongated cell morphology and F-actin structures were unchanged upon treatment with α-mangostin (Figs, 2,
208 3 and 4). Thus, the developed stress fibers in TIG-1 cells are relatively stable against α-mangostin. HeLa cells
209 have weak stress fibers and numerous protrusions and microvilli, and their surface stiffness is moderately
210 enhanced by the presence of actin structures (Figs. 3 and 4). The surface stiffness of HeLa cells was markedly
211 reduced, and the morphology appeared slightly shrunken, following the treatment with α-mangostin (Figs. 2
212 and 3). Thus, the weak actin structures with many protrusions and microvilli in HeLa cells were very sensitive
213 to α-mangostin. HEK293 cells have immature actin cytoskeletons, and as such, the mechanical stiffness of
214 HEK293 cells is very low (Figs. 3 and 4) [15]. Although the surface stiffness of HEK293 cells is slightly
215 decreased, it is difficult to evaluate the cell sensitivity to α-mangostin, since there is little room for decreasing
216 the stiffness to begin with. However, the morphology of HEK293 cells was also somewhat shrunken upon
217 treatment with α-mangostin, and therefore, they were most likely affected by α-mangostin (Fig, 2). RAW
218 264.7 cells did not display an extended morphology and exhibited F-actin at the cell-cell border and cortical
219 region with protrusions (Figs. 2 and 4). Also their surface stiffness was relatively low (Fig. 3). RAW 264.7

220 cells did not show any cell death after treatment with 100 μM of α-mangostin for 24 h (Fig. 1), and their
221 surface stiffness was hardly reduced (Fig. 3). Thus, RAW 264.7 cells were resistant to not only cytotoxic, but
222 also mechanical changes caused by of α-mangostin. The suspended KG-1 cells had cortical actin and
223 microvilli at the plasma membrane (Fig. 4) [33]. These cells were very sensitive to the cytotoxic effects of
224 α-mangostin and almost half of the cells died after treatment with 7.5 μM α-mangostin for 24 h (Fig. 1). Their
225 mechanical stiffness also markedly softened following the treatment with 5 and 10 μM of α-mangostin for 6 h
226 (Fig. 3). Thus, KG-1 cells and their actin structures were very sensitive to α-mangostin.
227 The impact of α-mangostin on the surface stiffness of HeLa and KG-1 cells was high compared to
228 other cell types (Fig. 3). On the other hand, the actin structures of these cells were different; for instance,
229 HeLa cells had many fine actin fibers inside the cells and KG-1 cells had cortical actin (Fig. 4). These actin
230 structures were not changed upon treatment with α-mangostin as observed in the images recorded by
231 conventional fluorescence microscopy (Fig. 4). How does α-mangostin reduce the mechanical stiffness of
232 these cells? Our previous study showed that the mechanical alteration determined by AFM was more sensitive
233 method to determine the actin changes in the cells than by fluorescence microscopy [19]. Thus, probably
234 micro-structures of actin cytoskeleton are changed by treatment with α-mangostin. HeLa cells and cancer
235 cells have many short microvillus and protrusions on their surface (Fig. 4) [14]. KG-1 cells are also covered
236 with short microvilli on the surface (Fig. 4) [33, 34]. Thus, the short microvillus structure of actin
237 cytoskeleton may be a sensitive target of α-mangostin. Microvilli structures are localized at the surface of
238 leukocytes as well [35-37]. If the actin microvilli are sensitive targets of α-mangostin, α-mangostin may also
239 affect the mechanical stiffness of circulating leukocytes.
240 Then, what kind of signal cascade or actin modulation molecules are the potential targets of
241 α-mangostin with respect to its effect on mechanical stiffness? Previous research work indicates that
242 α-mangostin has various contradictory functions on the molecules that affect the actin cytoskeleton; it inhibits
243 myosin light-chain kinase (MLCK) and cyclic AMP-dependent protein kinase (PKA) [38]; it increases myosin
244 light-chain (MLC) phosphorylation and induces Ca^{2+} influx in platelets [39]; it inhibits Ca^{2+}-ATPase in the

sarcoplasmic reticulum [40]; and it reduces Ca^{2+} elevation by suppressed Ca^{2+} influx [41]. These contradictory functions of α-mangostin can modulate the actin cytoskeleton positively and negatively. Thus, at present, it is difficult to assess the right targets of α-mangostin with respect to its effect on mechanical stiffness. But, recently, it has been reported that the mechanical stiffness and surface microvilli structures of KG-1 cells were related to cell adhesion and stimulation, and these were regulated by Ezrin/Radixin/Moesin (ERM) proteins that were linker proteins between membrane proteins and cortical actin [34]. In future, further studies using KG-1 cells might reveal the molecules involved in the processes of mechanical change caused by α-mangostin. The research will definitely help to better understand the complex and diverse functions of α-mangostin on various cells, including cancer cells, and enhance the pharmaceutical potential of naturally occurring compound α-mangostin.

RAW 264.7 cells did not display any cell death but demonstrated slight mechanical change brought about by α-mangostin (Figs. 1 and 3). Other studies have also reported that α-mangostin has no cytotoxic effect on RAW 264.7 cells but does inhibit NO and PGE2 production from lipopolysaccharide (LPS)-stimulated RAW 264.7 cells [32]. Furthermore, α-mangostin suppressed TLR4/NF-κB mediated inflammation reactions in LPS-stimulated RAW 264.7 cells [42]. Thus, although RAW 264.7 cells are completely resistant to the cytotoxic effects of α-mangostin, their intracellular molecules are affected by the multiple biological functions of α-mangostin.

Conclusions

In this study, we first reported that α-mangostin had a potential to reduce the mechanical properties of all cell types, including suspension cells, macrophages, and normal fibroblasts. The impact of α-mangostin on cell mechanical properties was found to be different from that of the cytotoxic effects on the cells. The surface stiffness of cancerous HeLa and floating KG-1 myeloblast cells was significantly softened by α-mangostin. In contrast, the surface stiffness of normal fibroblast TIG-1 and macrophage RAW 264.7 cells was slightly reduced by α-mangostin. Thus, the naturally occurring compound α-mangostin appears to modulate the

common signal cascades of the actin cytoskeleton inside these cells but further studies are needed to confirm this. Our findings will aid in the use of the complex and multi-functional α-mangostin in future medical applications.

Acknowledgements

This work was supported by JSPS KAKENHI Grant Number 16K01368 to T.K. and grant for Young Scientists, Institute of Environmental Science and Technology, The University of Kitakyushu to T.K.

Compliance with ethical standards

Conflict of Interest

The authors declare that they have no conflict of interest.

Human and Animal rights

This article does not contain any studies with human participants or animal performed by any of the authors.

References

1. Chen G, Li Y, Wang W, Deng L. Bioactivity and pharmacological properties of alpha-mangostin from the mangosteen fruit: a review. Expert Opin Ther Pat. 2018;28(5):415-27.
2. Watanapokasin R, Jarinthanan F, Nakamura Y, Sawasjirakij N, Jaratrungtawee A, Suksamrarn S. Effects of alpha-mangostin on apoptosis induction of human colon cancer. World J Gastroenterol. 2011;17(16):2086-95.
3. Kaomongkolgit R, Chaisomboon N, Pavasant P. Apoptotic effect of alpha-mangostin on head and neck squamous carcinoma cells. Arch Oral Biol. 2011;56(5):483-90.
4. Lee CH, Ying TH, Chiou HL, Hsieh SC, Wen SH, Chou RH et al. Alpha-mangostin induces apoptosis through activation of reactive oxygen species and ASK1/p38 signaling pathway in cervical cancer cells. Oncotarget. 2017;8(29):47425-39.
5. Hung SH, Shen KH, Wu CH, Liu CL, Shih YW. Alpha-mangostin suppresses PC-3 human prostate carcinoma cell metastasis by inhibiting matrix metalloproteinase-2/9 and urokinase-plasminogen expression through the JNK signaling pathway. J Agric Food Chem. 2009;57(4):1291-8.
6. Lee YB, Ko KC, Shi MD, Liao YC, Chiang TA, Wu PF et al. alpha-Mangostin, a novel dietary xanthone, suppresses TPA-mediated MMP-2 and MMP-9 expressions through the ERK signaling pathway in MCF-7 human breast adenocarcinoma cells. J Food Sci. 2010;75(1):H13-23.
7. Shih YW, Chien ST, Chen PS, Lee JH, Wu SH, Yin LT. Alpha-mangostin suppresses phorbol 12-myristate 13-acetate-induced MMP-2/MMP-9 expressions via alphavbeta3 integrin/FAK/ERK and NF-kappaB signaling pathway in human lung adenocarcinoma A549 cells. Cell Biochem Biophys. 2010;58(1):31-44.
8. Pedraza-Chaverri J, Reyes-Fermin LM, Nolasco-Amaya EG, Orozco-Ibarra M, Medina-Campos ON, Gonzalez-Cuahutencos O et al. ROS scavenging capacity and neuroprotective effect of alpha-mangostin against 3-nitropropionic acid in cerebellar granule neurons. Exp Toxicol Pathol. 2009;61(5):491-501.
9. Phan TKT, Shahbazzadeh F, Pham TTH, Kihara T. Alpha-mangostin inhibits the migration and invasion of A549 lung cancer cells. PeerJ. 2018;6:e5027.
10. Dai J, Sheetz MP. Mechanical properties of neuronal growth cone membranes studied by tether formation with laser optical tweezers. Biophys J. 1995;68(3):988-96.
11. Collinsworth AM, Zhang S, Kraus WE, Truskey GA. Apparent elastic modulus and hysteresis of skeletal muscle cells throughout differentiation. Am J Physiol Cell Physiol. 2002;283(4):C1219-27.
12. Guilak F, Erickson GR, Ting-Beall HP. The effects of osmotic stress on the viscoelastic and physical properties of articular chondrocytes. Biophys J. 2002;82(2):720-7.
13. Trickey WR, Vail TP, Guilak F. The role of the cytoskeleton in the viscoelastic properties of human articular chondrocytes. J Orthop Res. 2004;22(1):131-9.
14. Haghparast SM, Kihara T, Shimizu Y, Yuba S, Miyake J. Actin-based biomechanical features of suspended normal and cancer cells. J Biosci Bioeng. 2013;116(3):380-5.
15. Haghparast SM, Kihara T, Miyake J. Distinct mechanical behavior of HEK293 cells in adherent and suspended states. PeerJ. 2015;3:e1131.
16. Matzke R, Jacobson K, Radmacher M. Direct, high-resolution measurement of furrow stiffening during division of adherent cells. Nat Cell Biol. 2001;3(6):607-10.
17. Kunda P, Pelling AE, Liu T, Baum B. Moesin controls cortical rigidity, cell rounding, and spindle morphogenesis during mitosis. Curr Biol. 2008;18(2):91-101.
18. Fletcher DA, Mullins RD. Cell mechanics and the cytoskeleton. Nature. 2010;463(7280):485-92.
19. Shimizu Y, Haghparast SM, Kihara T, Miyake J. Cortical rigidity of round cells in mitotic phase and suspended state. Micron. 2012;43(12):1246-51.
20. Radmacher M, Fritz M, Kacher CM, Cleveland JP, Hansma PK. Measuring the viscoelastic properties of human platelets with the atomic force microscope. Biophys J. 1996;70(1):556-67.
21. Rotsch C, Braet F, Wisse E, Radmacher M. AFM imaging and elasticity measurements on living rat liver macrophages. Cell Biol Int. 1997;21(11):685-96.
22. Haga H, Sasaki S, Kawabata K, Ito E, Ushiki T, Sambongi T. Elasticity mapping of living fibroblasts by AFM and immunofluorescence observation of the cytoskeleton. Ultramicroscopy. 2000;82(1-4):253-8.
23. Kihara T, Haghparast SM, Shimizu Y, Yuba S, Miyake J. Physical properties of mesenchymal stem cells

are coordinated by the perinuclear actin cap. Biochem Biophys Res Commun. 2011;409(1):1-6.
24. Kagiwada H, Nakamura C, Kihara T, Kamiishi H, Kawano K, Nakamura N et al. The mechanical properties of a cell, as determined by its actin cytoskeleton, are important for nanoneedle insertion into a living cell. Cytoskeleton (Hoboken). 2010;67(8):496-503.
25. Shimizu Y, Kihara T, Haghparast SM, Yuba S, Miyake J. Simple display system of mechanical properties of cells and their dispersion. PLoS One. 2012;7(3):e34305.
26. Cross SE, Jin YS, Lu QY, Rao J, Gimzewski JK. Green tea extract selectively targets nanomechanics of live metastatic cancer cells. Nanotechnology. 2011;22(21):215101.
27. Ramos JR, Pabijan J, Garcia R, Lekka M. The softening of human bladder cancer cells happens at an early stage of the malignancy process. Beilstein J Nanotechnol. 2014;5:447-57.
28. Kihara T, Nakamura C, Suzuki M, Han S-W, Fukazawa K, Ishihara K et al. Development of a method to evaluate caspase-3 activity in a single cell using a nanoneedle and a fluorescent probe. Biosensors and Bioelectronics. 2009;25(1):22-7.
29. Kim KS, Cho CH, Park EK, Jung MH, Yoon KS, Park HK. AFM-detected apoptotic changes in morphology and biophysical property caused by paclitaxel in Ishikawa and HeLa cells. PLoS One. 2012;7(1):e30066.
30. Kato K, Umezawa K, Funeriu DP, Miyake M, Miyake J, Nagamune T. Immobilized culture of nonadherent cells on an oleyl poly(ethylene glycol) ether-modified surface. Biotechniques. 2003;35(5):1014-21.
31. Hertz H. Über die berührung fester elastischer Körper. J reine und angewandte Mathematik. 1881;92:156-71.
32. Chen LG, Yang LL, Wang CC. Anti-inflammatory activity of mangostins from Garcinia mangostana. Food Chem Toxicol. 2008;46(2):688-93.
33. Ohnishi H, Sasaki H, Nakamura Y, Kato S, Ando K, Narimatsu H et al. Regulation of cell shape and adhesion by CD34. Cell Adh Migr. 2013;7(5):426-33.
34. Tachibana K, Ohnishi H, Ali Haghparast SM, Kihara T, Miyake J. Activation of PKC induces leukocyte adhesion by the dephosphorylation of ERM. Biochemical and biophysical research communications. 2020;523(1):177-82.
35. von Andrian UH, Hasslen SR, Nelson RD, Erlandsen SL, Butcher EC. A central role for microvillous receptor presentation in leukocyte adhesion under flow. Cell. 1995;82(6):989-99.
36. Majstoravich S, Zhang J, Nicholson-Dykstra S, Linder S, Friedrich W, Siminovitch KA et al. Lymphocyte microvilli are dynamic, actin-dependent structures that do not require Wiskott-Aldrich syndrome protein (WASp) for their morphology. Blood. 2004;104(5):1396-403.
37. Yamane J, Ohnishi H, Sasaki H, Narimatsu H, Ohgushi H, Tachibana K. Formation of microvilli and phosphorylation of ERM family proteins by CD43, a potent inhibitor for cell adhesion: cell detachment is a potential cue for ERM phosphorylation and organization of cell morphology. Cell Adh Migr. 2011;5(2):119-32.
38. Jinsart W, Ternai B, Buddhasukh D, Polya GM. Inhibition of wheat embryo calcium-dependent protein kinase and other kinases by mangostin and gamma-mangostin. Phytochemistry. 1992;31(11):3711-3.
39. Liu Y, Park JM, Chang KH, Chin YW, Lee MY. alpha- and gamma-mangostin cause shape changes, inhibit aggregation and induce cytolysis of rat platelets. Chem Biol Interact. 2015;240:240-8.
40. Furukawa K, Shibusawa K, Chairungsrilerd N, Ohta T, Nozoe S, Ohizumi Y. The mode of inhibitory action of alpha-mangostin, a novel inhibitor, on the sarcoplasmic reticulum Ca(2+)-pumping ATPase from rabbit skeletal muscle. Jpn J Pharmacol. 1996;71(4):337-40.
41. Itoh T, Ohguchi K, Iinuma M, Nozawa Y, Akao Y. Inhibitory effect of xanthones isolated from the pericarp of Garcinia mangostana L. on rat basophilic leukemia RBL-2H3 cell degranulation. Bioorg Med Chem. 2008;16(8):4500-8.
42. Tao M, Jiang J, Wang L, Li Y, Mao Q, Dong J et al. alpha-Mangostin Alleviated Lipopolysaccharide Induced Acute Lung Injury in Rats by Suppressing NAMPT/NAD Controlled Inflammatory Reactions. Evid Based Complement Alternat Med. 2018;2018:5470187.

Figure captions

Fig. 1. Cytotoxicity of α-mangostin on TIG-1, HeLa, HEK293, RAW 264.7, and KG-1 cells. These cells were treated with various concentrations of α-mangostin (0 - 100 μM) and incubated for 24 h. The viable cells were measured using the cell counting kit-8. The values were calculated from 3 experiments. The effective concentration (EC_{50}) is shown in each graph.

Fig. 2. Phase contrast micrographs of TIG-1, HeLa, HEK293, RAW 264.7, and KG-1 cells treated with α-mangostin. These cells were cultured with or without 10 μM of α-mangostin (AMG) for 6 h. The object at the left of each micrograph is the AFM cantilever. Bar: 100 μm.

Fig. 3. Young's modulus of cells treated with α-mangostin. Young's modulus of TIG-1, HeLa, HEK293, RAW 264.7, and KG-1 cells were examined by AFM. The distribution of the Young's modulus of cells treated with α-mangostin for 6 h is represented by scatterplots. Each point represents the median value of 25 measuring points in each cell, and the Young's modulus in each condition is represented in more than 21 independent cells. The logarithmic average value of the Young's modulus (kPa) is shown at the top of each plot. # $p < 0.01$ vs. Young's modulus of the control (*Dunnett* pairwise comparison test).

Fig. 4. Fluorescence microscopy images of F-actin of cells treated with α-mangostin. TIG-1, HeLa, HEK293, RAW 264.7, and KG-1 cells were treated with 10 μM of α-mangostin (AMG) for 6 h or 2 μg/mL of cytochalasin D (CD) for 1.5 h, and then stained with rhodamine labeled-phalloidin. Bar: 50 μm.

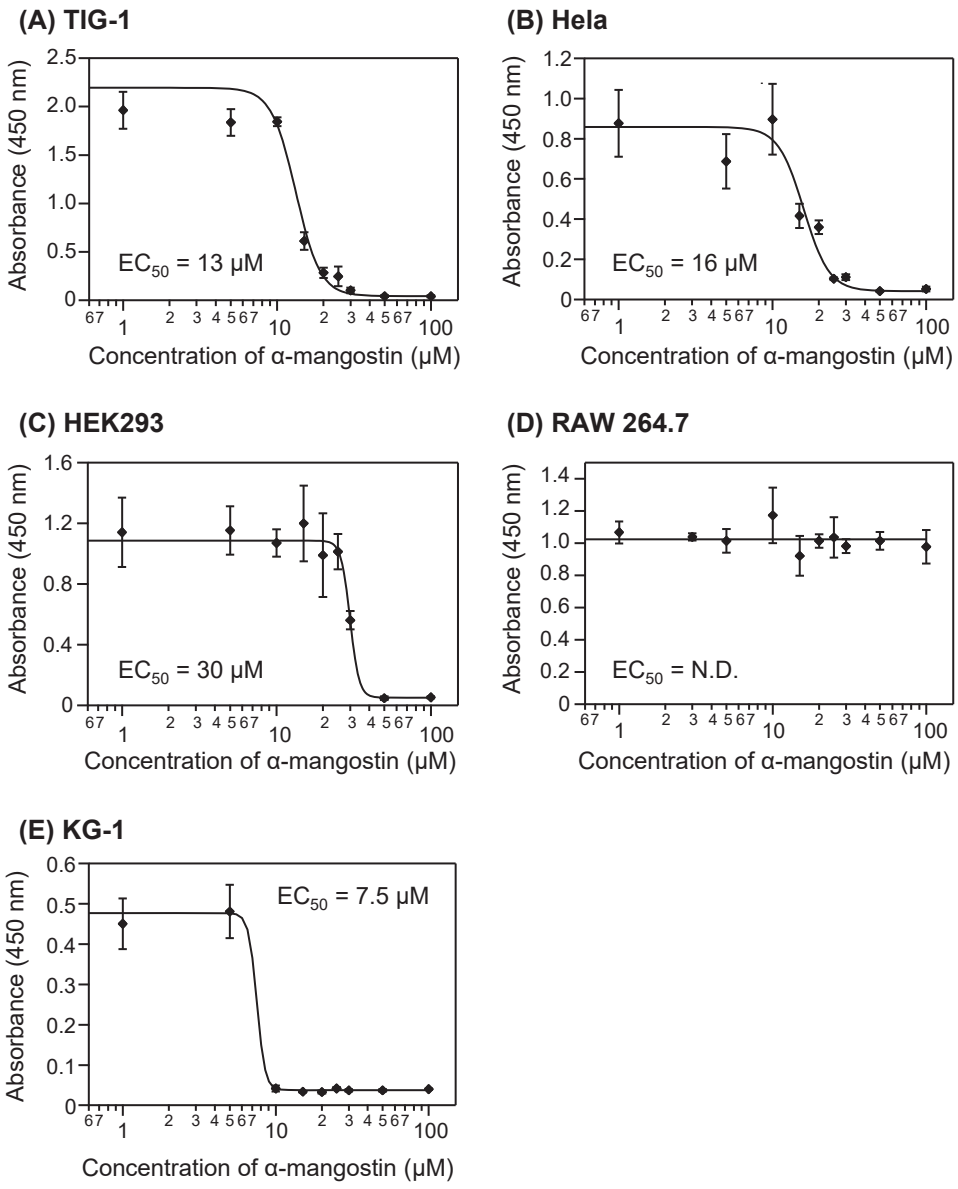

Fig. 1 Phan et al.

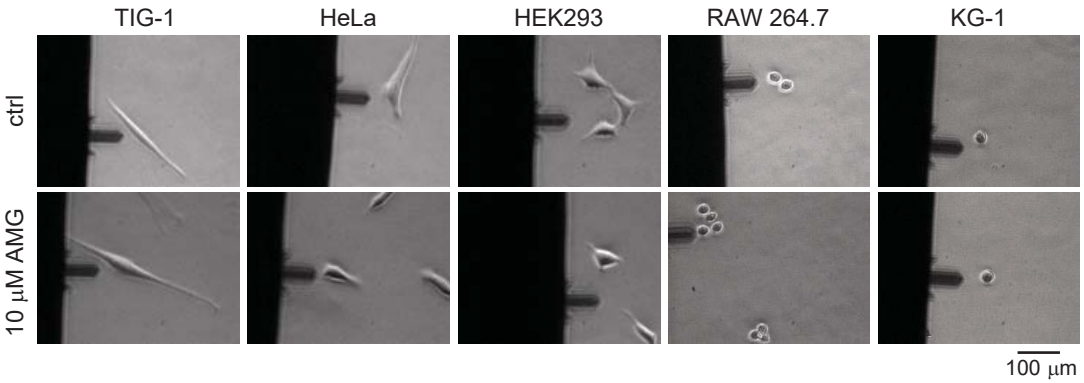

Fig. 2 Phan et al.

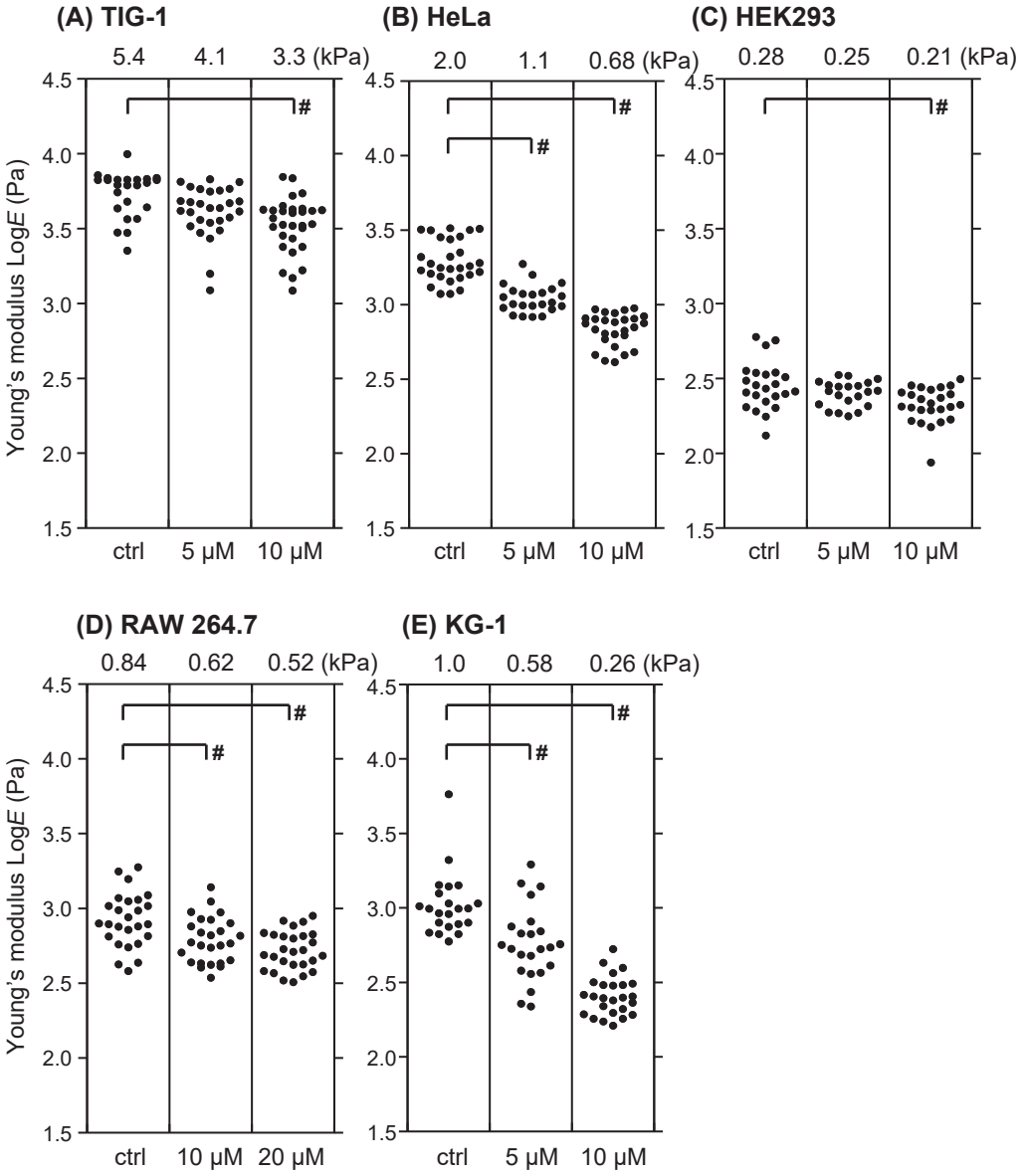

Fig. 3 Phan et al.

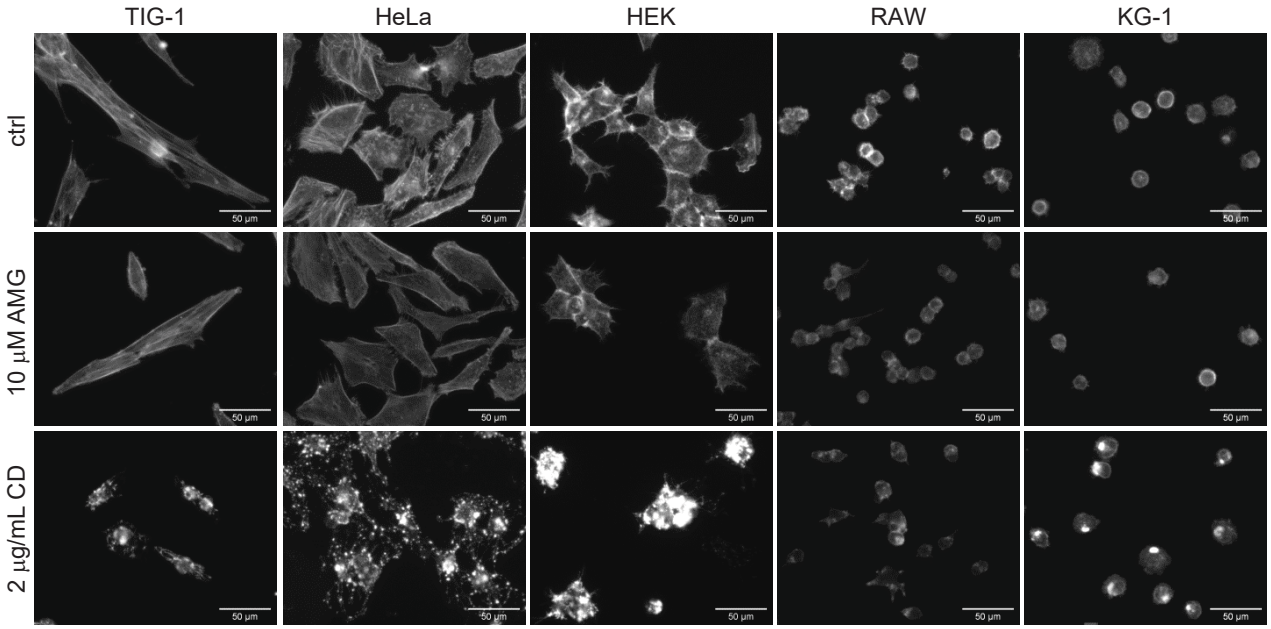

Fig. 4 Phan et al.